Ultimate tensile measurements of filled gelatin gels

Simon B. Ross-Murphy* and Susan Todd
Unilever Research, Colworth Laboratory, Sharnbrook, Bedford MK44 1LQ, UK
(Received 9 June 1982; revised 5 August 1982)

Ultimate tensile measurements were performed on the model system of glass filled gelatin gels. By using a range of sizes of glass ballotini, and also shape sorted fragments of fractured ballotini (denoted 'cubes') at varying phase volume of filler, the effect of size, shape and phase volume on the ultimate tensile properties of the filled gel samples was investigated. By constructing a force–extension failure envelope, a relationship was developed which enabled all the fracture data for the samples to be simply related, and this empirical relation was within experimental error identical to previously derived theoretical treatments of the dependence of small deformation modulus on phase volume.

Keywords Gelatin gel; composite gel; failure envelope; tensile testing; glass reinforced composites

INTRODUCTION

In a recent publication[1] we discussed in some detail the properties of gelatin gels modified by the incorporation of powdered glass filler into the sol, followed by gelation. In particular we discussed the effect of the phase volume, shape and size of filler particles upon the small deformation shear storage and loss moduli, and their ratio, the damping factor of tan δ. As a natural extension to this work we have now considered the effect of the same particulate phase factors upon the ultimate tensile properties of filled gelatin gels, in particular of the force to break and the extension to break, at different extension rates.

The effect of particulate phase volume, and particle shape has been extensively reviewed, the most recent reviews include those by Manson and Sperling[2], Lipatov[3], Bucknall[4] and Chow[5]. The majority of the experimental data in the literature seem to be concentrated upon the reinforcement of glassy matrix, presumably because of the commercial interest in glass fibre reinforced resins. More recently elastomers loaded with inorganic filler have attracted more interest—such systems are used in the technology of solid fuel propellants and, of course, there is considerable expertise in colloidal graphite/rubber composites. However, the amount of data in which the effect of filler particle size and shape has been examined in gels is surprisingly limited, and the present work provides some insight into filler effects in the particle size range of 15–500 microns.

EFFECT OF PARTICULATE PHASE VOLUME ON ULTIMATE TENSILE PROPERTIES

In the simplest treatment of the mechanical properties of rubbery composites it is assumed, firstly, that whilst the matrix is extensible, the disperse phase is completely non-extensible, and secondly that there is perfect adhesion between the phases at all tensile strains. Under these conditions, the actual strain ϵ' induced in the rubbery matrix is greater than the nominal strain $\epsilon(\phi)$, by a factor which depends upon the phase volume of filler. Thus if the effective strain to break is assumed to be constant, the nominal strain to break will decrease as φ, the filler phase volume increases[6]. At the same time, the small deformation tensile modulus $E(\varphi)$ increases as φ increases, so that the stress to break $\sigma_B (\simeq E(\varphi).\varepsilon(\varphi))$ can either increase or decrease with increasing φ, depending upon the relative relationships of $E(\varphi)$ and $\varepsilon(\varphi)$ to φ.

To illustrate this, *Figure 1* shows the behaviour of $\sigma_r = \sigma_B/\sigma_0$, with σ_0 the stress to break of the matrix phase, firstly if we assume that $E(\varphi) \propto (1-\varphi)^{-5/2}$ (after Landel[7]), $\epsilon(\phi) \propto 1-\phi^{1/3}$ [6] and that $\sigma_r = E(\phi).\epsilon(\phi)$. In this case, when φ is less than ~ 0.42, the tensile stress to break is lower than for the unmodified matrix, whereas for $\varphi \gtrsim 0.42$ σ_r is increased. Note that whilst the Landel relationship[7] is not

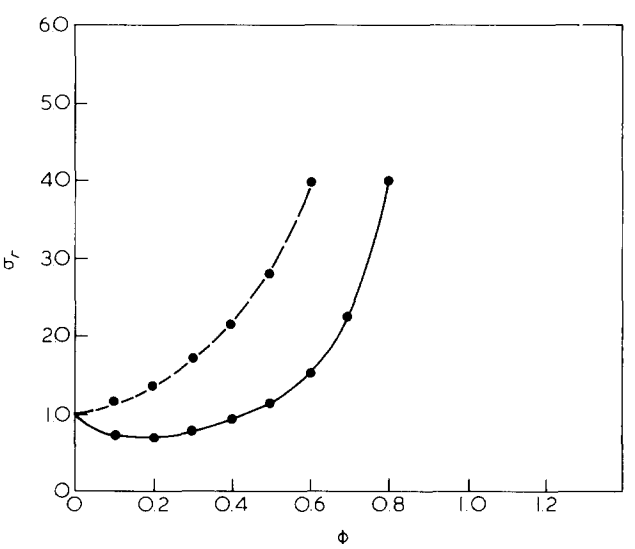

Figure 1 Relative stress to break for a filled system, σ_r, plotted against volume fraction ϕ of filler. Broken line $\sigma_r = (1-\phi)^{-3/2}$; solid line $\sigma_r = (1-\phi)^{-5/2}.(1-\phi^{1/3})$ (see text for details)

* All proof and correspondence to this author.

0032-3861/83/040481-06$03.00

necessarily the best fit to the observation variation of $E(\varphi)$ with φ, and the van der Poel[8,9] relation is usually adopted for spherical particles, the latter is not available in such a convenient arithmetic form, so here we have used the Landel form for illustration.

The relation $\epsilon(\phi) \propto 1-\phi^{1/3}$ assumes perfect adhesion between matrix and filler. A number of other treatments have argued that for non-adhesion $\epsilon(\phi) \propto S^1(1-\phi)$, where S^1 is a 'stress concentration' factor, which is experimentally found to be close to a half[10]. However, the simpler expression with $S^1=1$ is adopted here, giving $\sigma_r \sim (1-\varphi)^{-3/2}$, and in this case the stress to break σ_r is always increased compared with the result for the unfilled matrix (broken line), in other words the stress to break increases monotonically with φ.

All the above treatments however neglect the packing of the filler particles; for any shape of particles there is a maximum packing fraction φ_{max}, above which the filler particles are in contact with one another so that glass 'network' is formed, i.e. the filler and matrix phases are inverted. φ_{max} depends upon the geometry of the particulate phase, decreasing if the particles are changed from spheres to plates to needles. Samples with $\varphi > \varphi_{max}$ are effectively phase inverted gelatin in glass dispersions, and have no coherence. This means that as φ is increased towards φ_{max}, there is a maximum in, for example, small deformation modulus (see e.g. ref. 1).

At the same time there is a dependence of φ_{max} on size and size distribution. Such effects are usually small compared to the effect of shape, but for a bimodal distribution of spheres, in which smaller spheres can fit into the interstices between packed larger spheres, φ_{max} can be substantially increased over the hexagonal close packing φ_{max} of $\simeq 0.74$. Experimentally we find slightly lower values than this[1], typically for the spherical particles $\varphi_{max} \sim 0.64$.

EXPERIMENTAL

Preparation of samples

The gelatin used in this study was supplied by Croda as Croda boned 250 acid gelatin. This had a nominal Bloom strength of 250 and the concentration used was 20% by weight. This provided sufficient viscosity to prevent sedimentation of the glass filler particles during cooling and gelation.

Samples were prepared by dispersing the gelatin into cold water and heating to 65°C until dissolved. Water lost by evaporation was replaced and the solution transferred to screw top bottles which were placed in water at approximately 60°C to allow deaeration to occur.

The glass filler particles were supplied by Jencons Scientific Ltd., Hemel Hempstead, in the form of glass beads and milled glass cullet. The glass beads used were of different size grades denoted Grade 20 to Grade 8, Grade 20 being the smallest. (Details of the particle size and size distributions can be found in *Table 1*). The glass cullet was used as a supply of anisotropic, non regular shaped particles. This was sieved in order to narrow the size range of particles and material passing through a 125 μ sieve was collected. Very small 'dust' particles were removed by the use of an air classifier.

Knowing the densities of the glass and gelatin gel ($2.9\,g\,cm^{-3}$ and $1.05\,g\,cm^{-1}$ respectively) given phase volumes were prepared by mixing weighed quantities of the glass into the gelatin solution.

The sample was stirred to remove incorporated air and homogeneously distribute the glass particles. The sample was then cooled to approximately 38°C and uniform, thin slabs of gelatin were prepared by pouring the material onto a thick rigid metal plate. A top plate was pressed into position on to spacers which determined the sample thickness (3 mm). The plates were encompassed by a metal tray which retained excess material squeezed out from the plates. This was placed in a refrigerator for approximately 5 min to aid gelation of the gelatin. On removal from the refrigerator the samples were allowed to stand, between the plates, for 1 h before the specimens were cut.

A dumb-bell shaped cutter was used to prepare the specimens for testing. The cutter produced a sample which was 135 mm long × 30 mm wide at the ends. In the narrowed region, the geometry was 60 mm × 12.5 mm, and midway along this section a semicircular notch, 2 mm radius was produced. Each sample was stored overnight prior to testing in a dessicator modified such that the humidity prevented water loss from the samples. It was apparent that the rheological properties of the system were time dependent therefore, a careful routine of preparation, storage and testing was followed to minimise errors and problems of irreproducibility.

Although this treatment is not usually regarded as sufficient to reach a true equilibrium for gelatin gels, small deformation measurements had indicated that the effect of allowing greater time to equilibrate was effectively minimal.

Tensile testing

An Instron Universal Tester, Model 1122 was used to perform the tensile tests. The specimens were attached between the jaws which in turn were attached to the moveable crosshead and fixed load cell, such that the gap between the jaws was 8.0 cm. The system was calibrated using known weights.

Traces of force recorded as a function of time were obtained as the sample was extended. Four crosshead speeds were used, 1, 10, 100 and 1000 mm/min. Ambient temperature (22°C) was used as the excessive vibration of the sample (caused by the fan in the temperature controlled chamber) could be detected by the recorder.

RESULTS AND DISCUSSION

Despite precautions being taken, early experiments indicated that un-notched dumb-bell shaped specimens of filled gelatin failed extremely unpredictably under tension, sometimes at the clamps, and even sometimes tearing longitudinally—evidence of their low yield stress compared to bulk polymer systems. This effect was more pronounced in early experiments where the thickness of the sample (nominally 3 mm) varied more than in later work. Although alternative sample geometries such as

Table 1 Particle size and size distributions

	*d*3,0 (mean volume diameter)	Range (μ*)
Grade 20	38.6	15–80
13	109	70–190
11	181	110–260
8	550	440–780

* $1\mu = 10^{-6}$ m

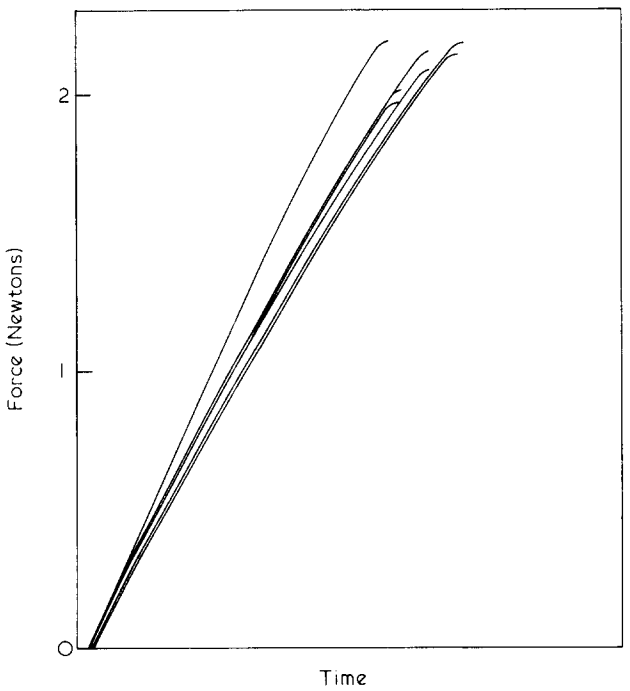

Figure 2 Force vs. time traces for various replicate samples of filled gels; the extension rate is constant

rings and ovals could be used[11] it was decided to notch the samples in a standard way at the mid-point of the specimen. For this reason the cutter was modified to include a notch cutter as described above. Although this ensured that the sample failed at the same region, it makes the stress difficult to estimate. It is also, of course, difficult to assess the strain for dumb-bell samples without using an external extensometer. For this reason all results are plotted in terms of 'experimental units', i.e. force and extension, rather than stress and strain.

Figure 2 shows typical force vs. time traces at constant extension rate, $\dot{\varepsilon}$ for a series of replicate samples. The force to break F and extension to break ε were 2.06 ± 0.09N and 6.2 ± 0.5 cm respectively. In these traces, the samples appear to fail without yielding.

For each sample then there is a corresponding pair of F and ε values, and each sample is a replicate of others (say 3–6) under the same conditions of extension rate, filler phase volume, size and shape of filler particles. Adopting the nomenclature familar to the statistician, each record (pair of F and ε values) is a replicate of a particular treatment, and each treatment is made up of a number of factors (e.g. $\dot{\varepsilon}$, φ etc.) each of which can take a number of levels (e.g. $\dot{\varepsilon}$ has four levels viz, 1, 10, 100, 1000 mm min^{-1}). To investigate the overall effect of each factor, and its significance, one could then carry out an analysis of variance and also consider any interactions between factors. Alternatively, although less rigorously, one can *a priori* neglect any possible interactions between factors and merely consider the effect of different levels of each factor, with the levels of all other factors held the same. This seems to be the approach adopted in much of the literature, and we illustrate the approach below. *Figure 3* shows the relative extension to break ε_r defined to be $\varepsilon_\phi/\varepsilon_0$ plotted against volume fraction φ. Here ε_ϕ is the extension to break of a system filled with particles at volume fraction φ, and ε_0 for the corresponding value for the unmodified gelatin gel. The data points are for the smallest spheres, and $\dot{\varepsilon}$ is 100 mm/min. The two lines correspond to the possible bounds $\varepsilon_r = 1 - \varphi^{1/3}$ and $\varepsilon_r = 1 - \varphi$ (cf *Figure 1* and ref. 12).

As can be seen the data follow neither of these curves very closely, initially lying above the upper line, but falling below as φ approaches the experimental φ_{max} of 0.64. The theories are largely inappropriate, since the curvature of the data appears to be convex. In any case, samples prepared with $\varphi > \varphi_{max}$ could be said to fail at very small absolute extensions, i.e. $\varepsilon_r \sim 0$. Note that we have assumed here that extension to break $\varepsilon_r \propto \sigma_B$, the true strain to break. Clearly this is true only as $\phi \rightarrow 0$, but even correcting for this would only partly improve the agreement with experiment, and would not predict $\varepsilon_r \rightarrow \sigma_B \rightarrow 0$ as $\phi \rightarrow \phi_{max}$, rather than $\phi \sim$ unity. The effect of particle size and shape is also neglected insofar as this affects φ_{max} and further experiments carried out at different extension rates clearly show the tendency of ε_r to increase with increasing $\dot{\varepsilon}$.

A further alternative approach to the all factor analysis of variance, or single factor treatments is to construct the full 'failure envelope'. As originally suggested by T. L. Smith[13,14], stress to break and strain to break for samples of an elastomer are plotted against one another logarithmically, at different strain rates and temperatures.

In this work we used a modified failure envelope, as explained below. *Figure 4* shows data of force to break plotted logarithmically against extension to break for every sample containing the Grade 20 spheres, and also for the unfilled gelatin (replicate batches). Each datum represents a separate test, and within each data set the spread of points represents both the scatter of replicates for any particular experiment (treatment), and also the effect of extension rate. The latter is indicated by the diagonal spread of the data points within any particular set. At the highest extension rate, 10^3 mm/min, a sample tends to fail at a larger extension, and with a greater force to break (even though the time to break $t_B = \varepsilon/\dot{\varepsilon}$ decreased) than at the slower rates. However the differences, for example, between data collected at the two slowest rates, 1 mm/min and 10 mm/min are largely masked by the scatter within each data set.

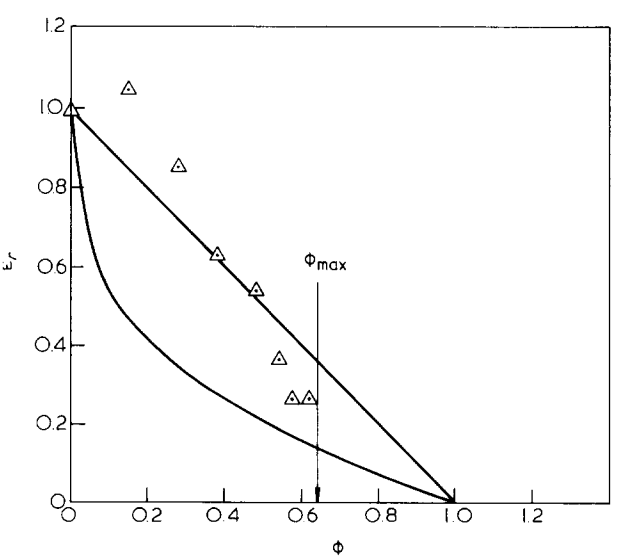

Figure 3 Relative extension to break, ε_r vs. ϕ. Triangles represent data for Grade 20 spheres (average values of 3–6 replicates) $\dot{\varepsilon} = 100$ mm min^{-1}. Upper line $\varepsilon_r = 1 - \phi$; lower line $\varepsilon_r = 1 - \phi^{1/3}$

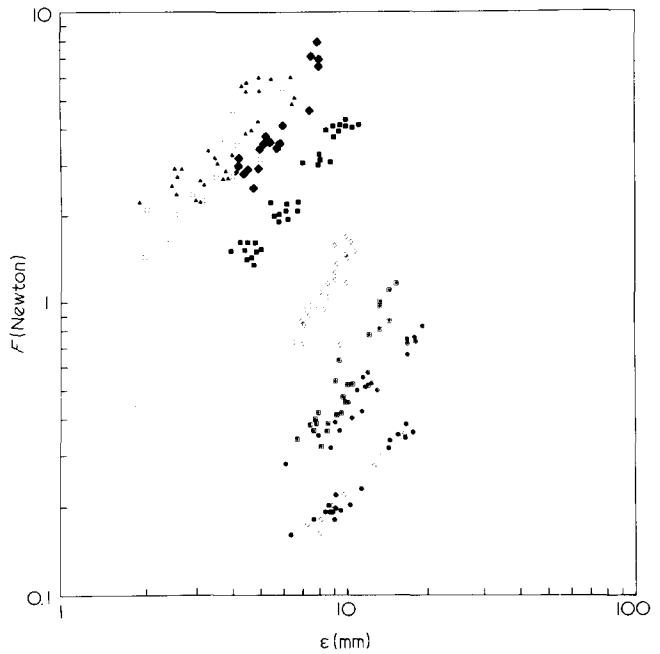

Figure 4 Force to break F against extension ε to break for filled and unfilled gelatin gels; Grade 20 spheres. ○ ●, unfilled; ⊙, ϕ =0.144; ⊡, ϕ=0.290; ◇, ϕ=0.380; ■, ϕ=0.480; ⊡, ϕ=0.540; ▲, ϕ=0.580; □, ϕ=0.630

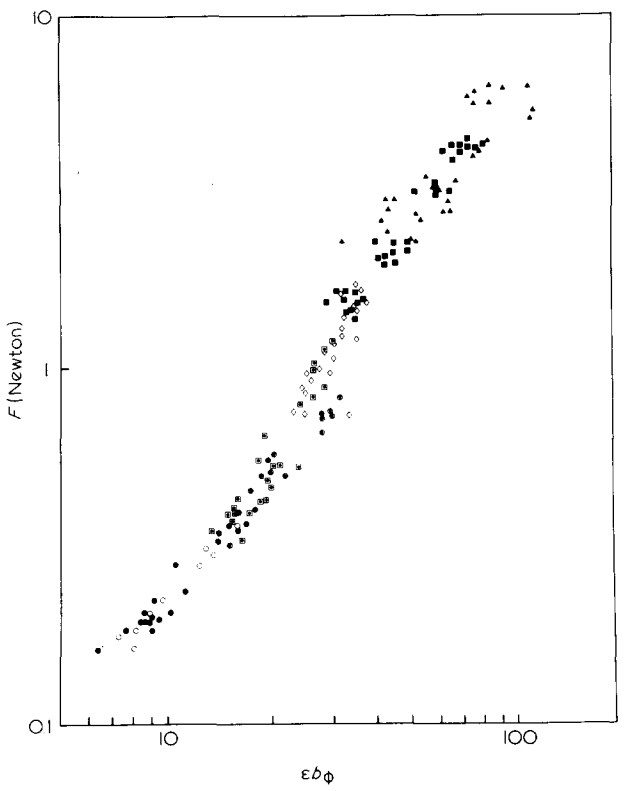

Figure 5 F plotted against $b_\varphi E$; failure envelope. Symbols as *Figure 4*. b_φ as in *Figure 6*

Figure 4 shows that the data collected for samples containing different volume fractions of filler produce a series of diagonal clusters, which are almost parallel, but shifted relative to one another—the effect of increasing φ is generally to decrease ε but to increase F.

By multiplying the extension ε by a shift factor b_ϕ, (i.e. by shifting all the data of *Figure 4* laterally), a common curve may be obtained as in *Figure 5*. Further this shift factor is not purely arbitrary, but mirrors the superposition of data collected at different temperatures onto a single time–temperature axis in the free volume treatments of Williams, Landel and Ferry[15], and T. L. Smith[14]. In more detail, as a rubbery elastomer is cooled below its glass transition temperature T_g, it becomes much more brittle, the strain to break decreases dramatically from say 200–500% to 1–2%, but the stress to break increases typically by a factor of 10^3–10^4. In molecular terms[16], the free volume available to the elastomer is decreased as the temperature is decreased. Evidence from our small deformation measurements[1] indicates that both G', the storage modulus, and $\tan\delta$, the loss tangent, increase substantially as φ approaches φ_{max}, the latter presumably as extra mechanisms for dissipation of heat and elasticity are introduced[16]. In these terms the increase in φ is equivalent to a decrease in temperature. The small deformation viscoelastic properties would suggest that the increase in filler volume fraction has made the gel more glassy. At the same time the addition of glass produces a strain magnification effect, the net contribution being reflected in the shift along the strain axis required to convert *Figure 4* to *Figure 5*.

Figure 6 shows the shift factor b_ϕ (which to make the product εb_ϕ dimensionless is defined to have units of mm^{-1}) plotted against φ. The line is that from the theoretical treatments of van der Poel[8] and J.C. Smith[9] for the dependence of the small deformation modulus upon the volume fraction of filler (for a recent derivation

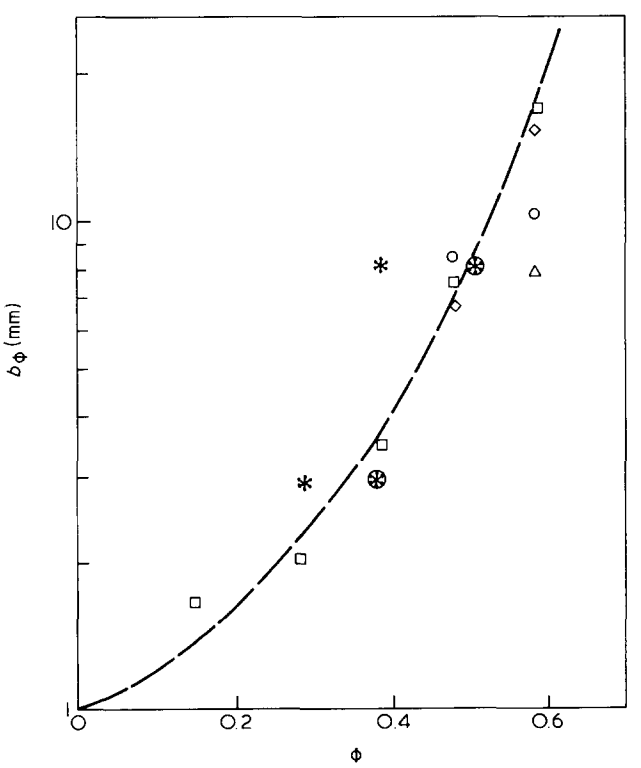

Figure 6 Failure shift parameter, b_ϕ, plotted against ϕ for different types of filler. Grade 20 spheres, □, Grade II spheres, ● ϕ_{max} ≃ 0.64; Grade 13 spheres, ◆; Grade 8 spheres, △; *, irregular shaped glass (ϕ_{max} ≃ 0.51); ◐ irregular shaped glass, $\phi_S = \phi_m \times 0.64/0.51$; ϕ_s= volume fraction scale to ϕ/ϕ_{max}; ϕ_m=measured volume fraction

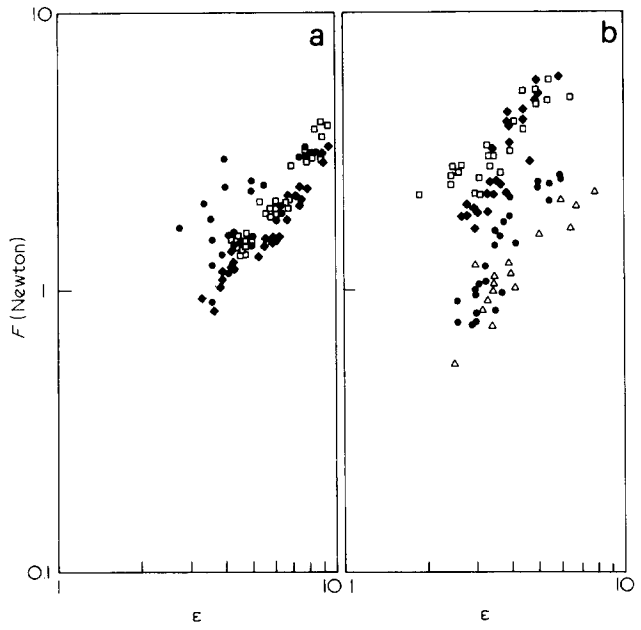

Figure 7 Effect of particle size, F vs. ε; □, Grade 20 spheres; ◆, Grade 13 spheres; ●, Grade 11 spheres; △, Grade 8 spheres. (a) $\phi = 0.482$ ($\phi/\phi_{max} = 75\%$); (b) $\phi = 0.580$ ($\phi/\phi_{max} = 91\%$)

of this model see ref 17). Interestingly the dependence of small deformation modulus upon φ is, within experimental error, the same as that of b_ϕ upon φ.

Figure 6 also shows the shift factors required to superpose force–extension failure envelopes for gelatin reinforced with non-regular shaped glass filler (this is the shape sorted fraction we denoted 'cubes', in inverted commas, in earlier work). The effect of changing from spherical filler phase ($\phi_{max} \approx 0.64$) to the 'cubes', with $\varphi_{max} \approx 0.51$ is clearly seen, but this effect is, gratifyingly, closely reflected in the ratio 0.64/0.51 (= 1.255) of these maximum packing fractions. By multiplying the volume fraction of 'cubes' by 1.255 to rescale the data to φ_{max}, the values of b_ϕ for these samples also lie close to the theoretical small deformation line. In other words, the data for different volume fractions and for two different shapes of particles may be rescaled to give a common curve. The generality of this observation remains to be tested for filler particles of very low φ_{max}, such as glass rods. In our small deformation measurements we were able to mill and fractionate glass wool to obtain samples in the size range 50–200 μ. However the procedure can only be used to produce small quantities of samples (say 5 g), nowhere near sufficient to carry out these large deformation studies, and so in the present work we were restricted to spheres and 'cubes'.

Furthermore, only the spheres (ballotini) could be readily obtained in sufficient quantity and sufficient range of sizes to investigate the effect of particle size on the force–extension envelope; the specification of the grades and their size ranges are given in the experimental section and in *Table 1*—the largest particles in this study are denoted Grade 8, the smallest Grade 20.

The effect of particle size is apparently dependent upon the volume fraction (an example of the interaction between factors mentioned earlier), because for $\varphi \lesssim 0.5$, the difference in failure behaviour for samples with different grades of ballotini is quite small. *Figure 7* illustrates the force–extension to break behaviour at two different volume fractions for several different grades of ballotini. At $\varphi = 0.48$, the results for the Grade 20 ballotini (*Figure 7a*), fall almost between the larger Grade 11 and Grade 13 samples. The overall effect of particle size upon failure is difficult to predict, and such effects are usually small, often occurring as a consequence of dewetting. However there is at least some evidence that a large particle size is detrimental to ultimate properties[2], and at high volume fractions our results reveal the same trend (*Figure 7b*). Theoretical relationships are almost invariably derived by assuming that the distribution of particles is isotropic, but in practice some anisotropy may be developed since the sample takes a finite time to gel, and some sedimentation may occur.

That there is some effect of particle size as φ approaches φ_{max} is indicated by the data of *Figure 7b*, where $\varphi \sim 0.58$ ($\varphi/\varphi_{max} \simeq 0.91$). Whilst the data for Grade 20 and Grade 13 ballotini seem not to differ greatly, that for Grade 11 and Grade 8 filled samples are clearly different. To clarify this effect, the values of b_ϕ required to superpose all these results on the master curve of *Figure 5* are given in *Figure 6*, and as φ approaches φ_{max} it appears that b_ϕ decreases with increasing particle size. This is another form of the explanation above, but experimentally φ_{max} itself also decreases slightly with increasing particle size. In the case of a single spherical particle exactly surrounded by a cube, then φ_{max} is $\pi/6$ ($\simeq 0.52$), so this is an estimate of φ_{max} for a single macroscopic particle. Interestingly we have observed a similar deviation from ideality as $\varphi \rightarrow \varphi_{max}$ in the small deformation modulus[1], which lends more support for our strategy of relating ultimate tensile properties to small deformation measurements.

CONCLUSION

This work has investigated the effect of particle size, shape and volume fraction on the properties of a gelatin composite. The force–extension shift factor b_ϕ introduced, enabled a master failure envelope to be constructed, and the relationship of b_ϕ to φ was shown to be effectively the same as that due to van der Poel–Smith for small deformation modulus, independent of size for spheres up to $\varphi/\varphi_{max} \simeq 0.9$, and shape when data for the cubes were scaled to φ_{max}. In this way an important generalization of the results could be obtained, which it is hoped may be applicable to other gel composites.

ACKNOWLEDGEMENTS

Thanks are due to Miss B. Sadrani and Mrs. L. Linger for expert technical assistance and to Dr A. H. Clark and Mr. H. McEvoy for invaluable and stimulating discussions.

REFERENCES

1 Richardson, R. K., Robinson, G., Ross-Murphy, S. B. and Todd, S. *Polym. Bull.* 1981, **4**, 541
2 Manson, J. A. and Sperling, L. H. 'Polymer Blends and Composites', Plenum Press, New York, 1976
3 Lipatov, Yu. S. *Adv. Polym. Sci.* 1977, **22**, 1
4 Bucknall, C. B. *Adv. Polym. Sci.* 1978, **27**, 121
5 Chow, T. S. *J. Mater. Sci.* 1980, **15**, 1873

6 Nielsen, L. E. *J. Appl. Polym. Sci.* 1966, **10**, 97
7 Landel, R. F. *Trans. Soc. Rheology* 1958, **2**, 53
8 Van der Poel, C. *Rheol. Acta.* 1958, **1**, 198
9 Smith, J. C. *J. Res. Natl. Bur. Stand.* 1975, **79A**, 419
10 Leidner, J. and Woodhams, R. T. *J. Appl. Polym. Sci.* 1974, **18**, 1639
11 Myers, F. A. and Wenrick, J. D. *Rubber Chem. Technol.* 1974, **47**, 1213
12 Piggott, M. R. and Leidner, J. *J. Appl. Polym. Sci.* 1974, **18**, 1619
13 Smith, T. L. *J. Polym. Sci.* 1963, **A1**, 3597
14 Smith, T. L. in 'Rheology Vol. V', (Ed. F. R. Eirich), Academic Press, N.Y., 1969
15 Williams, M. L., Landel, R. F. and Ferry, J. D. *J. Am. Chem. Soc.* 1955, **77**, 3701
16 Ferry, J. D. 'Viscoelastic Properties of Polymers', John Wiley, New York, 3rd Edition, 1980
17 Christensen, R. M. 'Mechanics of Composite Materials', John Wiley, New York, 1979